INVESTIGATION OF SURFACE POTENTIAL ASYMMETRY IN PHOSPHOLIPID VESICLES BY A SPIN LABEL RELAXATION METHOD

STEVEN A. SUNDBERG AND WAYNE L. HUBBELL
Department of Chemistry, University of California, Berkeley, California 90024

ABSTRACT In earlier work, Castle and Hubbell (1976) demonstrated the use of a spin-labeled amphiphile as a probe for the electrostatic potential at the outer surface of charged phospholipid vesicles. In recent experiments, we have shown that the hydrophobic anion tetraphenylboron (TPB) promotes transbilayer migration of the probe molecule. Relaxation data recorded following the rapid mixing of the probe with TPB-containing vesicle samples provides information about the electrostatic potentials at both the outer and inner vesicle surfaces. The measured potentials for both surfaces of asymmetrically screened vesicles were found to be in good agreement with theoretical values calculated using their known surface charge density. The method is also sensitive to transmembrane potentials as indicated by the response of the label to potentials created with the use of potassium concentration gradients and valinomycin.

INTRODUCTION

Electrostatic potentials in biological membranes modulate many phenomena including ion transport and surface-surface interactions. In structures containing membranes in close apposition, such as chloroplast grana and photoreceptor cell outer segments, surface electrostatic potentials are particularly important determinants of the overall structure. In the photoreceptor the separation of the inner surfaces within a disk membrane compartment is only ~30 Å (Chabre and Cavaggioni, 1973). At such close approach, electrostatic interaction should be considerable and an estimate of the potential at the disk membrane internal surface is an important step in the analysis of the forces between the membrane surfaces.

A number of physical-chemical approaches have been developed to investigate electrical potentials near, within, and across biological membranes (see Wagonner, 1979; McLaughlin, 1977; and Cafiso and Hubbell, 1981 for reviews). Castle and Hubbell (1976) and Gaffney and Mich (1976) showed that amphiphilic spin labels such as *N,N*-dimethyl-*N*-nonyl-*N*-tempoyl ammonium bromide (I), shown below, could be used to estimate surface potentials at the outer surface of phospholipid vesicles.

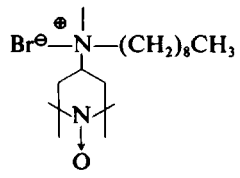

(I)

In this method, the partition coefficient of (I) between the membrane surface and bulk aqueous phase is determined from the electron paramagnetic resonance (EPR) spectrum of (I) in equilibrium with a charged membrane surface, and the surface potential relative to the bulk phase determined directly from this partition coefficient. The approach is restricted to the outer membrane surface simply because the spin label (I) is very membrane impermeable in phospholipid vesicles and partition equilibrium is rapidly established only with the outer surface.

In this paper we describe experiments that extend this technique to the study of potentials at both the outer and inner surfaces, i.e., to the study of membrane surface charge asymmetry. The principle of the method is straightforward. Trace amounts of the hydrophobic anion tetraphenylborate (TPB) catalyze the transmembrane migration of (I). Therefore, a rapid mixing experiment in which (I) is mixed with vesicles containing trace amounts of TPB will result in time dependent spectral changes reflecting the transmembrane migration of (I) and the corresponding increase of membrane surface area seen by the probe. The spectral information at $t = 0$ after the mix is analyzed to give the external surface potential while the combined information from $t = \infty$ and $t = 0$ gives the internal surface potential.

Unlike phospholipid vesicles, native membranes are relatively permeable to (I), and transmembrane relaxation processes can be observed without the aid of TPB. In such instances, the relaxation kinetics can also give information regarding the charge density asymmetry.

MATERIALS AND METHODS

Materials

The spin-labeled quaternary ammonium molecule, *N,N*-dimethyl-*N*-nonyl-*N*-tempoylammonium bromide, was synthesized as described pre-

Dr. Sundberg's permanent address is Albert Einstein School of Medicine, Department of Anatomy, Bronx, NY
Dr. Hubbell's current address is Jules Stein Eye Institute, UCLA School of Medicine, Los Angeles, CA 90024

viously (Hubbell et al., 1970). Egg phosphatidylcholine (PC) was isolated from fresh eggs according to the procedure of Singleton et al. (1965). The final product yield for the lipid isolation was determined by phosphorous analysis as described by Bartlett (1959) and the lipid was stored in chloroform under argon at −20°C. Egg phosphatidic acid (PA) was purchased form Calbiochem-Behring (La Jolla, CA). Sodium TPB was purchased from the Aldrich Chemical Company (Milwaukee, WI). Gramicidin D and Valinomycin were obtained from Sigma Chemical Company (St. Louis, MO).

Preparation of Phospholipid Vesicles

Stock solutions of the lipids, stored in chloroform under argon at −20°C, were warmed to room temperature before opening. Samples of egg PC containing the desired mole fraction of PA were prepared and brought to dryness in a rotary evaporator. The samples were then placed under vacuum (~0.2 mm Hg) for at least 12 h to remove residual traces of solvent. Following resuspension in an aqueous buffer, the lipid was sonicated under argon at 0°C for 30 min with a Heat Systems-Ultrasonics (Plainview, NY) sonifier until the solution became translucent. The vesicle solutions were then centrifuged at 31,000 *g* for 20 min to remove titanium particles produced by the sonifier tip and small quantities of poorly sonicated lipid. Vesicle stock solutions were sonicated at lipid concentrations of 8% (wt/vol) and then diluted for use in ESR experiments. Final lipid concentrations were determined by phosphorus assay (Bartlett, 1959).

Vesicles formed from egg PC or egg PC containing 8 mol % PA had average diameters of 280 ±50 Å and 280 ±70 Å, respectively, as determined by negative stain electron microscopy (Castle and Hubbell, 1976). We assume these vesicles to be spherical in suspension since they are near the limiting radius of curvature (Huang and Mason, 1977) and Cafiso and Hubbell (1978*a*) showed that the experimentally determined vesicle internal volume was accounted for by a spherical structure. The lipid concentrations and vesicle sizes were used to determine V_o/V_i, the ratio of external/internal volumes. For vesicles of 280 Å diameter, V_{mo}/V_{mi}, the ratio of external/internal volumes of membrane surface binding domains is 2.4 (Cafiso and Hubbell, 1978*a*).

Sample Preparation for EPR Measurements

For most of the surface potential measurements described below, stock solutions of PC or 8 mol % PA in PC vesicles prepared in 20 mM MOPS, 30 mM NaCl, pH 7.0 (referred to hereafter as "buffer"), were diluted to a lipid concentration of ~1.6% (wt/vol) for PC or 0.8% (wt/vol) for PC/PA vesicles before use in EPR experiments. The final lipid concentration of each vesicle sample was determined by phosphorous analysis. Tetraphenylboron and Gramicidin D were added to vesicle samples and allowed to equilibrate before carrying out rapid mixing experiments. External ionic conditions were manipulated by adding the appropriate salts to the quaternary ammonium solution before mixing.

For transmembrane potential experiments, vesicles were prepared in 50 mM MOPS, pH 7.0, containing 225 mM K_2SO_4. The vesicles were then passed through a BioGel A-0.5m (BioRad Labs, Richmond, CA) column as described previously (Cafiso and Hubbell, 1978*a*) to exchange the external solution for one containing lesser K_2SO_4 concentrations (total ionic strength was kept constant at 225 mM K_2SO_4 by adding the appropriate concentration of Na_2SO_4). Following the addition of 10 μM Valinomycin, the vesicle samples were allowed to equilibrate for at least 90 min before use. The equilibrium transmembrane potentials were computed as previously described (Cafiso and Hubbell, 1978*a*).

Electron Paramagnetic Resonance Measurements

Unless otherwise stated, all EPR experiments were carried out using a final spin label concentration of 20 μM and ~ 0.8% (wt/vol) lipid for PC vesicles and 0.4% (wt/vol) for PC/PA vesicles. Electron spin resonance spectra were recorded with a Varian E-line EPR spectrometer operating in the X-band frequency range.

Rapid mixing experiments were carried out using a pneumatically driven plunger mechanism holding two syringes, one containing the quaternary ammonium solution, and the other containing the vesicle sample. The syringes were connected to a mixing port on the front end of a flow-through quartz sample cell positioned in the spectrometer cavity. The mixing time was ~40 ms (Cafiso and Hubbell, 1982). The spectrometer was tuned to the high field line of the nitroxide spectrum and the amplitude of that peak was monitored as a function of time following the mixing of the probe with the vesicle sample.

Analysis of Electron Paramagnetic Resonance Spectra

In the presence of phospholipid vesicles, the EPR spectrum of (I) consists of both free and membrane bound spin label populations (Castle and Hubbell, 1976). The ratio of the number of spin labels bound to the number free, λ , is related to the EPR spectral amplitude by

$$\lambda = N_b/N_f = \frac{(A_f^\circ - A)}{A - (\beta/\alpha)A_f^\circ}, \quad (1)$$

where N_b and N_f are the numbers of spin labels bound and free, respectively, A_f° is the amplitude of the high-field spectral line in the absence of membranes, β and α are constants relating the spectral amplitudes to the actual numbers of spins and A is the total amplitude of the high-field line in the presence of membranes. The value of β/α is found to be −0.035 for (I) in egg PC bilayers (Sundberg, 1983).

The effective partition coefficient λ is thus determined by a single spectral variable, the amplitude of the high-field line, A. This feature makes it possible to follow time-dependent changes in the partition coefficient simply by following the time-dependence of the amplitude A. The actual high field EPR signal amplitude due to the free population alone, A_f, is related to the total high field amplitude A according to

$$A_f = \frac{A - \beta/\alpha\, A_f^\circ}{1 - \beta/\alpha}. \quad (2)$$

The difference between A and A_f is only significant when a large fraction of (I) is membrane bound. Even for 75% bound, A_f differs from A by only 3%. The derivation and assumptions underlying this analysis have been previously discussed (Cafiso and Hubbell, 1981).

THEORY AND RESULTS

Signal Relaxation Induced by TPB

As previously shown, phospholipid bilayers are very impermeable to spin label (I), which has a half-time for permeation in egg PC vesicles of ~14 h (Castle and Hubbell, 1976). Thus, when (I) is rapidly mixed with phospholipid vesicles, partition equilibrium is established at the outer surface within the mixing time (~40 ms) and the spectral amplitude A remains constant over the time domain explored in the present experiments (~10 min).

On the other hand, inclusion of μM concentrations of TPB in the vesicle suspension results in relatively rapid decrease of A to a new stable value following the mix (Fig. 1 *a*). The decrease in A with time is not due to chemical reduction of the nitroxide, but is the result of an increase in the bound population of (I) at the expense of the free population due to a transmembrane migration process of

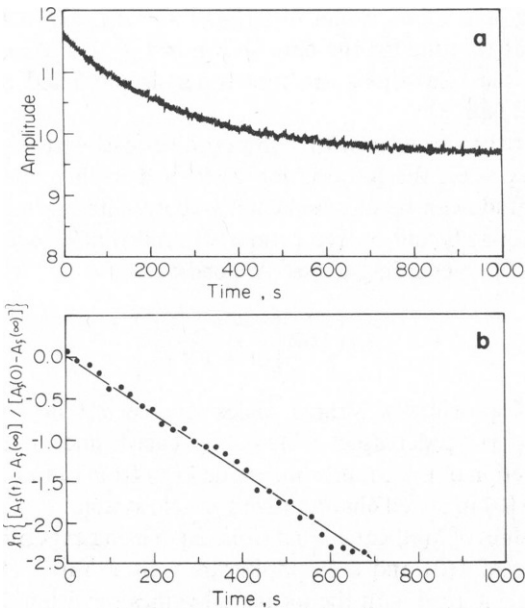

FIGURE 1 EPR signal amplitude relaxation of (I) following mixing with phospholipid vesicles. (*a*) Tracing of high-field spectral amplitude, in arbitrary units, as a function of time after mixing. (*b*) Semilogarithmic plot of data in part *a* showing first-order kinetic behavior over approximately three half-lives. For this data, <50% of the spin label is bound. Under these conditions A and A_f differ by only a few percent and they have been taken to be equal in calculating the points in *b* from the data in *a*. The vesicles were formed from 0.5% (wt/vol) egg PC in buffer and contained 5 μM TPB, and 10 μM gramicidin D. The total concentration of (I) was 20 μM. At this lipid concentration, $V_o/V_i = 391$. The EPR high-field signal amplitude in the absence of membranes was 19.75 in the same amplitude units used in the figure. The equation for the least-squares exponential fit to the data in part *a* is $A = 1.94\, e^{-0.0037t} + 9.64$.

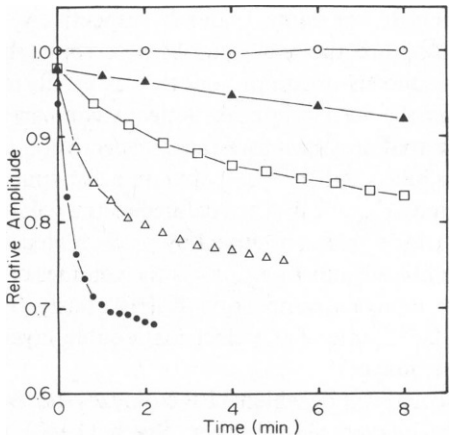

FIGURE 2 Effect of TPB concentration on the transmembrane relaxation rate of spin label (I). The relative amplitudes of the high-field resonance of (I) are plotted as a function of time after mixing with vesicles in the presence of various concentrations of TPB. The vesicles were formed from 0.5% (wt/vol) egg PC in buffer and contained 10 μM gramicidin D with the following additions: 0 μM TPB, open circles; 2 μM TPB, closed triangles; 5 μM TPB, open squares; 10 μM TPB, open triangles; 20 μM TPB, closed circles. The total concentration of (I) was 20 μM.

the spin label.[1] The increase in bound population is simply the result of an increased amount of membrane binding surface available when (I) has access to the interior volume of the vesicle. Cafiso and Hubbell (1982) have studied similar time-dependent EPR amplitudes due to transmembrane migration of spin labeled phosphonium ions, and enhanced transmembrane transport of organic cations by TPB has been studied previously (Cafiso and Hubbell 1982; Stark, 1980).

The actual rate of transmembrane migration depends on the amount of TPB in the vesicle suspension as shown in Fig. 2. Note here that the initial amplitude at $t = 0$ is relatively constant and independent of the amount of TPB used up to 10 μM, corresponding to ~10 TPB per vesicle. This indicates that, as expected, these low levels of TPB do not significantly perturb the binding constant of (I) to the membrane surface. This also implies that significant complex formation between (I) and TPB does not occur at these low concentrations of TPB.

Relaxation Kinetics

The transport of molecules like (I) that have well-defined adsorption domains can be described by the kinetic scheme shown in Fig. 3. In this model, the spin label is assumed to be in partition equilibrium with the external and interior membrane surfaces with partition coefficients K_o and K_i, respectively. The inward and outward transmembrane transport steps are rate limiting and characterized by

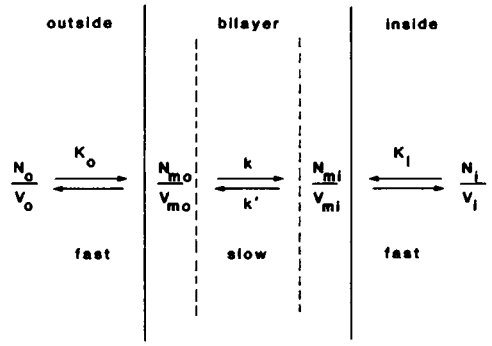

FIGURE 3 Three step transport model for transmembrane relaxation of spin label (I). V_{mo} and V_{mi} are the volumes of the bilayer phases occupied by spin labels giving rise to a "bound" EPR lineshape. V_o and V_i are the volumes of the outer and inner aqueous compartments. N_{mo}, N_{mi} and N_oN_i are the numbers of the spin labels occupying these compartments. k and k' are rate constants and K_o and K_i are equilibrium constants, each corresponding to the indicated process. The transmembrane step is assumed to be elementary and rate-limiting, while the surface processes are taken to be at equilibrium.

[1] The egg PC vesicles as prepared here contain few (if any) reducing equivalents for the nitroxide. For example, rapidly permeating analogues of (I) such as the secondary amine *N*-tempoyl-*N*-hexyl amine (Cafiso and Hubbell, 1978*b*) or the simple permeant nitroxide TEMPO give no spectral relaxation on the time scale of the mixing, and the amplitudes remain stable for periods much longer than those involved in the present experiments.

first-order rate constants k and k' respectively. N_o, N_{mo}, N_i, and N_{mi} are the mole numbers of spin label in the external aqueous medium, on the external membrane surface, in the vesicle interior aqueous compartment and on the internal membrane surface, respectively. N_o and N_i do not include double layer populations of spin label (I). The volumes V_{mo} and V_{mi} are defined as the volumes of the bilayer surface phases occupied by probe molecules bound to the membrane and V_o and V_i as the volumes of the outer and inner aqueous compartments (rigorously, V_o and V_i exclude the volume of the electrical double layer on each side of the bilayer).

The mechanism by which TPB catalyzes the transport of (I) across bilayers is unknown. Stark (1980) has some evidence suggesting that TPB forms an ion pair with organic cations at the membrane surface and hence acts as a carrier for the cation. Irrespective of the mechanism, TPB present at low concentrations simply acts to modify the apparent transmembrane rate constants, and the formal kinetic expressions describing the relaxation to equilibrium is the same as previously given for the relaxation of phosphonium ions (Cafiso and Hubbell, 1982),[2] and in terms of the free signal amplitude is

$$[A_f(t) - A_f(\infty)] = [A_f(0) - A_f(\infty)]e^{-\gamma t}, \quad (3)$$

where $A_f(t)$, $A_f(0)$, and $A_f(\infty)$ are the free signal amplitudes at time t, 0, and at equilibrium, respectively. $A_f(t)$ is calculated from the total observed amplitude according to Eq. 2. The dependence of the time constant γ on parameters of the model will depend on details of the transport mechanism in the presence of TPB and will in general be different from that given for the phosphphonium ion relaxation referred to above.

The amplitude of the relaxation, $[A_f(0) - A_f(\infty)]$, is related to the binding constants, surface potentials and vesicle geometrical parameters by

$$[A_f(0) - A_f(\infty)] = A_f^\circ\left[\frac{1}{1 + \frac{V_o\epsilon_o}{V_i\epsilon_i}}\right]\left[\frac{1}{\epsilon_o} - \frac{1}{\epsilon_i}\right], \quad (4)$$

where A_f° is the high field spectral amplitude in the absence of membranes and the functions ϵ_o and ϵ_i are

$$\epsilon_o \equiv 1 + \frac{V_{mo}}{V_o}K_o e^{-\phi_o}$$

$$\epsilon_i \equiv 1 + \frac{V_{mi}}{V_i}K_i e^{-\phi_i},$$

and ϕ_o and ϕ_i are the reduced surface potentials related to the actual surface potentials Ψ_o and Ψ_i by $\phi_o = \Psi_o ZF/RT$; $\phi_i = \Psi_i ZF/RT$.

[2]The kinetic expression given here is identical to that given by Cafiso and Hubbell except for the rate constants. Cafiso and Hubbell used rate constants k_f and k_r. These are related by k and k' given here by $k_f = k_1$ and $k_r = k_{-1}V_{mo}/V_{mi}$.

Fig. 1 *b* shows a plot of $\ln[A_f(t) - A_f(\infty)]/[A_f(0) - A_f(\infty)]$ vs. time for the data shown in Fig. 1 *a*. As can be seen, the relaxations are first order as predicted by the model (Eq. 3).

For the simple case of symmetric vesicles with $K_i = K_o$ and $\psi_i = \psi_o$, the information contained in the relaxation amplitude can be most succinctly represented in terms of the initial bound-to-free ratio $\lambda(0)$, and that at equilibrium, $\lambda(\infty)$, according to (see Appendix)

$$\lambda(\infty) = \lambda(0)\left[\frac{1 + V_{mi}/V_{mo}}{1 + V_i/V_o}\right]. \quad (5)$$

Eq. 5 provides a simple check of the validity of the transport model upon which it is based since it allows prediction of the equilibrium value $\lambda(\infty)$ from initial condition $\lambda(0)$ in a well characterized vesicle system.

Values of $\lambda(\infty)$ calculated from Eq. 5 using experimental values of $\lambda(0)$ and the appropriate volume ratios (Fig. 1 legend) agreed with the measured values to within 3% for uncharged, symmetric vesicles. For example, for the data shown in Fig. 1, $\lambda(0)$ is determined from the initial amplitude to be $\lambda(0) = 0.66$. The value of $\lambda(\infty)$, predicted by Eq. 5 and the above value of $\lambda(0)$ is $\lambda(\infty) = 0.94$. This compares well with the experimental value $\lambda(\infty) = 0.95$ calculated directly from the data in Fig. 1 *a*. There are no adjustable parameters in this calculation and the excellent agreement between calculated and experimental values lend support to the simple model of transport of (I) into topologically closed vesicles with well-defined compartments and apparently equal binding affinity to both surfaces.

Transmembrane Potentials from Equilibrium Partitioning Data

According to the scheme in Fig. 3, the equilibrium state of the system, described by $\lambda(\infty)$, should be a predictable function of the transmembrane potential, since the transport of (I) involves charge displacement across the membrane. The analysis of this situation is formally identical to that for the membrane-permeable phosphonium ion spin labels studied earlier (Cafiso and Hubbell, 1978*a*) and the relationship between the transmembrane potential, $\Delta\Psi_m$, and $\lambda(\infty)$ is given by

$$\Delta\Psi_m = \frac{RT}{ZF}\ln\left[\frac{\lambda(0)(V_{mi}/V_{mo}) - \lambda(\infty)(V_i/V_o)}{\lambda(\infty) - \lambda(0)}\right]. \quad (6)$$

Eq. 6 holds for vesicles with no surface charge asymmetry. As a test of the model, the relaxation of (I) across vesicles with an imposed transmembrane potential created by K^+ gradients and valinomycin was investigated.

Fig. 4 shows the transmembrane potentials computed from the spectral amplitude data according to Eq. 6 for several K^+ gradients as well as the theoretical equilibrium transmembrane potential as a function of K^+_{in}/K^+_{out} (solid curve), corrected for H^+ movement (Cafiso and

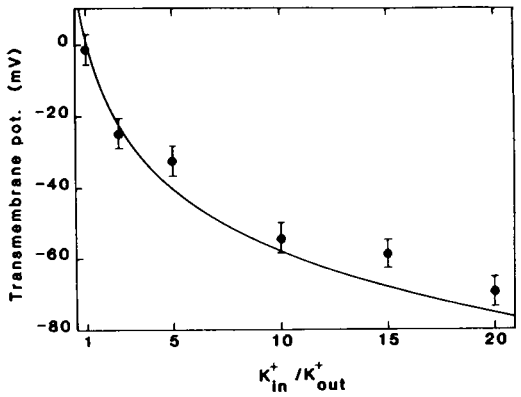

FIGURE 4 Transmembrane potential as a function of $[K^+]_i/[K^+]_o$. Transmembrane potentials at each K^+ gradient were computed from the relaxation data and Eq. 6 (solid points). The solid curve indicates the expected equilibrium K^+ potential. The error bars indicate mean uncertainty in measurements from four independent experiments.

Hubbell, 1978*a*). The agreement between prediction and experiment is tolerable and supports the simple charge transport model of Fig. 3.

Surface Potentials from Equilibrium Partitioning Data

Within the time of mixing of vesicles with (I), binding equilibrium is established with the external vesicle surface. The transport of (I) across the vesicle in the presence of micromolar amounts of TPB is sufficiently slow that such $t = 0$ data may be used to determine the binding constant to the external surface and hence the outer surface potential. The surface potential is determined from the partitioning data according to (Castle and Hubbell, 1976)

$$\phi_o = \ln \frac{\lambda(0)}{\lambda'(0)}, \tag{7}$$

where $\lambda(0)$ is the value of λ at $t = 0$ after the mixing and $\lambda'(0)$ is the value at $t = 0$ in the absence of a surface potential. In the present experiments $\lambda'(0)$ is obtained from PC vesicles containing no added PA and hence having no surface potential. Changes in the surface potential are measurable without knowledge of $\lambda'(0)$ according to

$$\Delta\phi_o \equiv \phi_o(2) - \phi_o(1) = -\ln \frac{\lambda_2(0)}{\lambda_1(0)}, \tag{8}$$

where $\phi_o(2)$ and $\phi_o(1)$ are two (reduced) surface potentials corresponding to different conditions (different charge densities or different salt concentrations) and $\lambda_2(0)$, $\lambda_1(0)$ are the corresponding partition coefficients for (I). This equation assumes constancy of $\lambda'(0)$. Eq. 8 is particularly valuable in studies of native membrane systems where determination of $\lambda'(0)$ is often difficult.

Castle and Hubbell (1976) studied the outer surface potential of PC/PA vesicles using (I) and showed that the dependence of the surface potential on concentration of NaCl was reasonably well described by the simple Gouy-Chapman equation with no correction for ion binding. In the present work, we employ both arginine hydrochloride and ammonium acetate as electrolytes, and to ensure that these electrolytes show simple screening behavior without binding, we have studied the surface potential of PC vesicles containing 8 mol % PA as a function of concentration for both electrolytes, and the results are shown in Fig. 5. The surface potentials were calculated from the values of $\lambda(0)$ in each salt concentration according to Eq. 7. The solid curve in Fig. 5 is the theoretical value of the surface potential calculated according to

$$2\sinh\left(\frac{\phi_o}{2}\right) + \frac{4}{A}\tanh\left(\frac{\phi_o}{4}\right) - \frac{\sigma\mathcal{F}}{RT\kappa\epsilon_o\epsilon_r} = 0, \tag{9}$$

where ϕ_o is the reduced potential defined above, σ is the surface charge density in C/m^2, ϵ_o is the permittivity of a vacuum and ϵ is the dielectric constant of the medium. $A = \kappa r$, where κ is the Debye constant and r is the vesicle radius in m. Eq. 9 is an accurate approximation to the exact solution of the nonlinearized spherical Poisson-Boltzmann equation derived by Ohshima et al. (1982).[3] The plot in Fig. 5 according to this equation is obtained

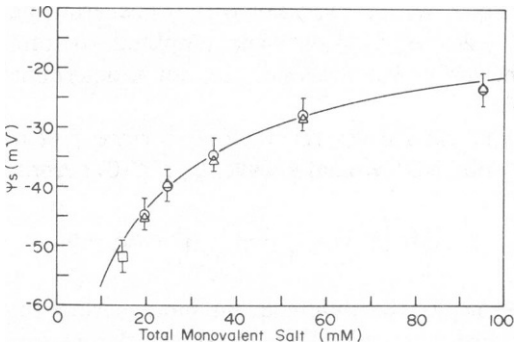

FIGURE 5 Arginine chloride and ammonium acetate screening of the outer surface potential. The surface potential of PC vesicles containing 8 mol % PA was determined from the binding of (I) at various concentrations of electrolyte. The vesicles were prepared from 0.3% (wt/vol) lipid in a buffer of 20 mM MOPS, pH = 7.0. The total concentration of (I) was 20 μM. Open circles, arginine chloride; open triangles, ammonium acetate; single open square, buffer alone with no addition (total ionic strength = 14.7 mM). The solid curve is the expected dependence of the potential on monovalent salt concentration assuming no ion binding (see text).

[3] In earlier work, we employed the Gouy-Chapman theory to provide a relationship between surface charge density and surface potential (Castle and Hubbell, 1976) since it provided a mathematically simple formulation. Although the Gouy-Chapman Eq. is derived on the basis of planar geometry, it gives values of the potential at the surface very close to those obtained from the spherical Poisson-Boltzmann Eq. as long as $\kappa r \gg 1$, a situation satisfactorily satisfied for sonicated vesicles at moderate salt concentrations. Since the relatively simple and highly accurate expression given by Eq. 8 has recently become available for the spherical geometry, we choose to employ it in preference to the more approximate Gouy-Chapman equation.

using $r = 140$ Å as determined from electron microscopy and $\sigma = 0.018\ C/m^2$, which corresponds to 8 mol % of charge assuming 70 $Å^2$ as the area occupied per phospholipid molecule in the surface. The fit is excellent and indicates that both arginine and ammonium ions act as ideal electrolytes with no apparent binding to surface groups. These are extremely useful electrolytes for membrane investigations since arginine is impermeable even to membranes that are leaky to Na^+, and ammonium acetate behaves as a completely permeable electrolyte. Thus this pair can be used in asymmetric screening experiments in vesicle systems.

We now turn to consideration of transmembrane relaxation of (I) across vesicles for which $\Delta\phi_m = 0$ and $\phi_i \neq \phi_o$. For the compositionally symmetric vesicles used here we will take $K_i \simeq K_o$, and for $\Delta\phi_m = 0$, the relationship between $\lambda(0)$ and $\lambda(\infty)$ is (see Appendix)

$$\ell n\left[\lambda(\infty) - \frac{\lambda(0)}{1 + V_i/V_o}\right] - \ell n\left[\frac{\lambda'(0)V_{mi}/V_{mo}}{1 + V_i/V_o}\right] + \phi_i = 0. \quad (10)$$

This equation together with Eq. 6 can be used to determine both the outer and inner surface potentials in one relaxation experiment. From the value of $\lambda(0)$ derived from the initial signal amplitude according to Eq. 1, one obtains ϕ_o using Eq. 7. With the value of $\lambda(0)$, the experimental value of $\lambda(\infty)$ derived from the signal amplitude at equilibrium and the various volume ratios, $\Delta\phi_i$ can be determined from Eq. 10.

Again, changes in the internal surface potential are readily obtained without knowledge of $\lambda'(0)$ according to

$$\Delta\left[\ell n\left(\lambda(\infty) - \frac{\lambda(0)}{1 + V_i/V_o}\right)\right] + \Delta\phi_i = 0, \quad (11)$$

where $\Delta\phi_i$ is the difference in inner surface potential corresponding to a change in either charge density or electrolyte concentration and the difference function is just the difference in the ℓn function for the two different conditions.

We have sought to test the method outlined above by measuring $\Delta\phi_o$ and $\Delta\phi_i$ in situations where known electrostatic asymmetries are created and systematically varied. Fig. 6 *a* shows the experimental changes in surface potential (according to Eqs. 8 and 11) induced by increasing the external concentration of the impermeable electrolyte arginine hydrochloride. It is clear that the external surface potential is screened by the added salt while the internal surface potential is unaffected, within experimental uncertainties. Fig. 6 *b* shows $\Delta\phi_o$ and $\Delta\phi_i$ induced by increasing concentrations of the membrane-permeable salt ammonium acetate. Here both the internal and external surfaces are being screened by the same amount within experimental error. The solid curves in Fig. 6 *a* and *b* are the predicted changes in potential according to Eq. 9. The data are thus reasonably well accounted for by the model presented above.

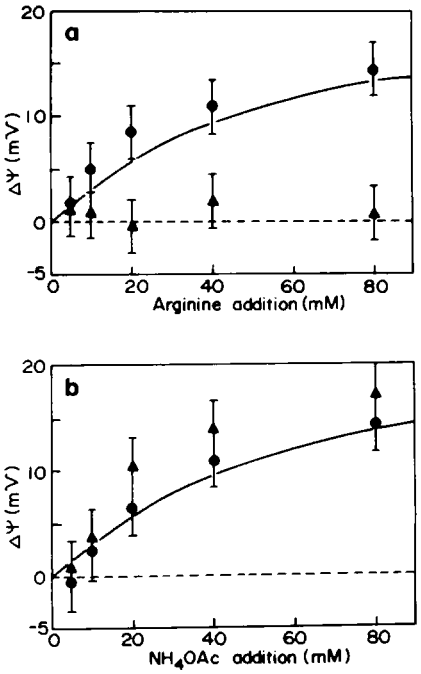

FIGURE 6 Surface potential changes as a function of external salt addition. (*a*) Addition of arginine hydrochloride. (*b*) Addition of ammonium acetate. Circles, outer surface potential changes; triangles, inner surface potential changes; both estimated by the spin label relaxation approach described in the text. The solid lines are the predicted potential changes in each case. The dashed lines indicate zero potential changes. The vesicles contained 8 mol % PA in PC and were prepared in buffer (total ionic strength = 42.7 mM). The vesicles also contained 10 μM gramicidin D and 5 μM TPB. Error bars indicate the estimated uncertainty in the individual measurements.

We have chosen to carry out this initial investigation of the method on sonicated phospholipid vesicles because they have been so well characterized. Nevertheless, their use has imposed certain constraints that limit the precision of the data. In particular, the internal vesicle volume is so small that the minimum ionic strength employed must be quite high so that the Debye length does not become of the order of the vesicle internal radius and lead to complications due to overlap of the internal double layers. This means that the changes in potential created by increasing the concentration of a 1:1 electrolyte are quite small (~15 mV max as shown in Fig. 6) with substantial relative uncertainties. Slight variations in $\lambda'(0)$ between different preparations due to lipid oxidation or other causes and relatively small errors in the determination of lipid concentration result in systematic shifts in the calculated potential/concentration curves of the order of a few millivolts. Since the changes we are observing are so small, we have chosen to plot changes in potential rather than absolute potential to eliminate the effect of these systematic sources of error.

The use of an impermeable 2:1 electrolyte to screen the outer surface potential and thus create an electrostatic asymmetry provides a somewhat improved situation due to

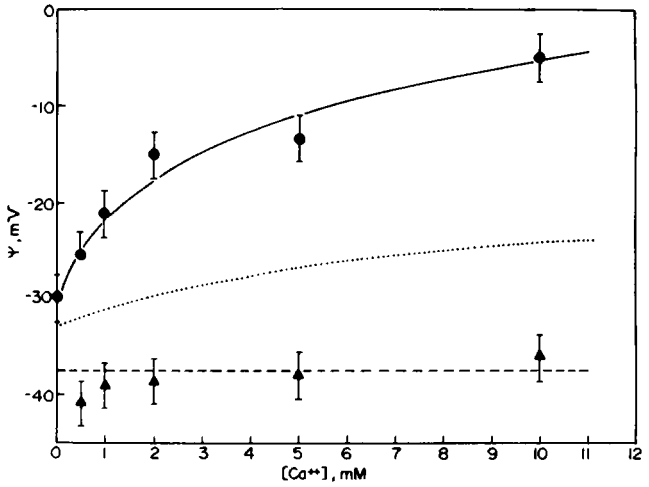

FIGURE 7 Surface potential as a function of $CaCl_2$ addition. Circles, outer surface potentials; triangles, inner surface potentials; both estimated by the spin label relaxation approach as described in the text. The solid curve indicates the theoretical potential profile for the outer surface calculated as discussed in the text and including Ca^{++} binding. The dotted curve is a theoretical potential profile for the outer surface without Ca^{++} binding. The dashed curve is the theoretical potential profile for the inner surface potential in the absence of Ca^{++} but with a charge density 20% higher than the outer surface (see text). The vesicles contained 8 mol % PA in PC, 10 μM gramicidin D and 5 μM TPB and were suspended in buffer.

the fact the potential changes are larger and can be produced by lower concentrations of electrolytes. Fig. 7 shows both Ψ_o and Ψ_i estimated from the partition coefficient of (I) according to Eqs. 7 and 10 as a function of added external $CaCl_2$. Again, it is seen that the external surface potential is screened efffectively while the internal surface potential remains essentially constant.

To compare this data with theoretical predictions, an accurate approximation to the exact solution of the nonlinearized spherical Poisson-Boltzmann Eq. for mixed 1:1 and 2:1 electrolytes has been employed and is given by (Ohshima et al., 1982).

$$pt + \frac{2}{Apt}\left\{\left[(3-p)t - 3 - \frac{3^{1/2}(1-\eta)}{2\eta^{1/2}}\right] \cdot \ln\left[\frac{1+(\eta/3)^{1/2}t-(\eta/3)^{1/2}}{1-(\eta/3)^{1/2}t+(\eta/3)^{1/2}}\right]\right\} - \frac{\sigma\mathcal{F}}{RT\kappa\epsilon_o\epsilon_r} = 0, \quad (12)$$

where

$$p = (1 - e^{-\phi_o})$$

$$t = [(1-\eta/3)e^{\phi_o} + \eta/3)]^{1/2}$$

$$\eta = 3C_2/(C_1 + 3C_2),$$

and C_1 and C_2 are 1:1 and 2:1 electrolyte concentrations, respectively. Other quantities are the same as in Eq. 9. For divalent ions, surface binding to both neutral and charged phospholipids is significant.

To account for ion binding, the charge density in Eq. 12 is given by (McLaughlin et al., 1981)

$$\sigma = \frac{-\mathcal{F}\sigma_{PA}\{1 - K_2[Ca^{++}]e^{-2\psi_o}\}}{1 + K_1[Na^+]e^{-\phi_o} + K_2[Ca^{++}]e^{-2\phi_o}} + \frac{\mathcal{F}\sigma_{PC}2K_3[Ca^{++}]e^{-2\phi_o}}{1 + K_3[Ca^{++}]e^{-2\phi_o}}, \quad (13)$$

where σ_{PA}, σ_{PC} are the surface concentrations of PA and PC in mols/m^2, K_1, K_2, K_3 are the association constants for Na^+, Ca^{++} to PA and Ca^{++} to PC respectively. Eisenberg et al. (1979) have found K_1 for Na^+ binding to PS to be $\sim 0.6\ M^{-1}$, and give data indicating that it is not too different for Na^+ binding to PA.

McLaughlin, A. et al. (1978) and McLaughlin, S. et al. (1981) have made a detailed investigation of the binding of divalent metal ions to bilayers formed from PC, PS, and their mixtures. For assumed 1:1 complex formation of Ca^{++} with phospholipid, these authors report binding constants of 12 M^{-1} for PS and 1–3 M^{-1} for PC. Since Barton (1968) has given evidence that the Ca^{++} binding constants to PA and PS are very similar, 12 M^{-1} will be used as a reasonable approximation for the 1:1 binding constant of Ca^{++} to PA.

The solid curve in Fig. 7 is a theoretical prediction of the outer surface potential as a function of Ca^{++} using values of $K_1 = 0.6\ M^{-1}$, $K_2 = 12\ M^{-1}$ and $K_3 = 1.3\ M^{-1}$.

The dotted curve in Fig. 7 is the predicted curve for no ion binding, i.e., simple screening, demonstrating the need for inclusion of ion binding to account for the data. The effect of Na^+ ion binding is rather small throughout, being

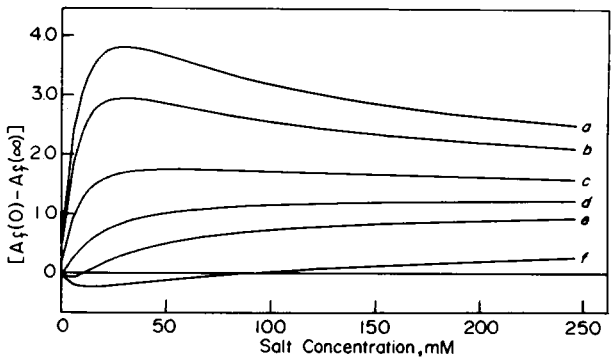

FIGURE 8 Salt dependence of the relaxation amplitude as a function of membrane charge asymmetry. Relaxation amplitudes were computed according to Eq. 4 and the following parameters: $V_o/V_i = 20$; $K_o V_{mo}/V_o = 0.1$; $K_i V_{mi}/V_i = 1.8$; $V_o/V_i = 20$. These values correspond to a 2 mg/ml suspension of bovine rod outer segment membrane vesicles of radius ~2,500 Å, but are considered typical. $A_f = 20$. Surface potentials required for the calculation of $[A_f(0) - A_f(\infty)]$ were obtained from given charge densities according to the Gouy-Chapman model. In each plot in the figure, the outer charge density on the vesicle surface was fixed at $\sigma_o = 2.56 \times 10^{-2}\ C/m^2$. This corresponds to ~160,000 charges/μ^2 of membrane surface and is not atypical of native membranes. The inner charge densities for the indicated curves above were: (*a*) $-3.20 \times 10^{-2}\ C/m^2$; (*b*) $-2.56 \times 10^{-2}\ C/m^2$; (*c*) $-1.60 \times 10^{-2}\ C/m^2$; (*d*) $-8.00 \times 10^{-3}\ C/m^2$; (*e*) $0\ C/m^2$; (*f*) $3.20 \times 10^{2}\ C/m^{-2}$.

maximal at 0 added Ca^{++} and amounting to a calculated reduction in potential of only ~ 2.5 mV (see Fig. 8). At Ca^{++} concentrations of 5 mM and higher, the effect is <1 mV.

The internal surface potential is essentially independent of added Ca^{++}. Note however, that the internal potential is more negative than the outer at 0 added Ca^{++} by ~10 mV. Although this is a relatively small difference, it is reproducibly observed and is apparently significant. The dashed line in Fig. 7 is computed according to Eq. 9, using a charge density given by Eq. 13 with $K_1 = 0.6$, $K_2 = K_3 = 0$ and a value for σ_{PA} 20% higher than for the external surface. The significance of this will be discussed below.

DISCUSSION

The primary objective of this work was to assess the utility of the spin label relaxation approach to estimation of transmembrane electrostatic asymmetry. To this end, a well-defined model system of sonicated phospholipid vesicles with an imposed electrostatic asymmetry was investigated. In the present experiments, membranes with approximately equal inner and outer charge densities were prepared and asymmetric surface potentials were generated via asymmetric ionic strengths. The results demonstrate that the relaxation of spin label (I) across membranes of phospholipid vesicles can be used to estimate both inner and outer surface potentials and, with a suitable theory, the charge densities at the inner and outer surfaces.

In applying the relaxation method for estimating surface potential asymmetries, it is important that the number of molecules of (I) that bind to the membrane be sufficiently small not to perturb the surface potential, and that the transmembrane potential be either short-circuited or buffered against changes due to the transmembrane flow of (I) during relaxation to equilibrium. The concentrations of (I) used in these experiments (~20 spin labels per vesicle of ~6,000 lipids) was sufficiently small to guarantee that changes in the surface potential due to binding of (I) did not exceed 1–2 mV. However, significant transmembrane potentials (of the order of 10–20 mV, interior positive) could develop as a result of permeation of (I). It is for this reason that 10 μM gramicidin has been included in all experiments. In the presence of Na^+ and/or a buffered H^+ concentration, this ionophore effectively short-circuits the membrane capacitance and maintains the vesicles at zero transmembrane potential. Failure to include the ionophore leads to significantly different results interpretable in terms of an interior positive transmembrane potential of the expected magnitude (Sundberg, 1983).

As shown in Fig. 7, the internal surface potentials calculated according to Eq. 10 were quite reproducibly ~10 mV more negative than the external surface potentials for symmetric ionic solutions. There are several possible explanations for this relatively small effect. The simplest is that the charge density on the inner surface is greater than that on the outer surface. This in fact would be expected even if the ratio of PA/PC were the same on both surfaces since the packing density and hence the charge density are greater on the inner surface of these small vesicles. Huang and Mason (1978) estimate the area per molecule on the inner surface to be ~20% smaller than that on the outer surface for sonicated egg PC vesicles. This would increase the charge density on the inner surface by ~20%. The dashed line in Fig. 7 is calculated for this situation. Clearly, the asymmetry in packing alone could account for the slight surface potential asymmetry. In addition, of course, there may actually be a slight asymmetry in the charged lipid distribution.

Another explanation to be considered is that the binding of (I) may be higher for the inner surface than for the outer surface. This would lead to the calculation of a too negative interior surface potential. This explanation is unlikely to be the correct one since results presented above showed that uncharged vesicles were quite symmetric with respect to binding of (I). This result is not expected to change due to the presence of small amounts of PA, since earlier results from Castle and Hubbell (1976) showed that the intrinsic binding constant of (I) was independent of the amount of PA present up to 8 mol %.

Finally, it should be pointed out that the surface potential at a concave surface is expected to be of larger magnitude than that for the same charge density at a convex surface. Such geometrical effects, however, are only important at ionic strengths lower than those employed here. It thus seems most likely that the apparent asymmetry in surface potential is real and due to a surface charge density asymmetry.

The relaxation method described above can be directly applied to vesicles derived from native membrane systems. In fact, such vesicles will pose fewer problems than the sonicated phospholipid vesicles. For example, the typically much larger size of native membrane vesicles will permit examination of low internal ionic strengths without concern about the overlap of the internal double layer.

Native membrane vesicles will also turn out to be more convenient to study, since the permeability to (I) is much higher than for phospholipid vesicles and eliminates the need for TPB as a carrier. For example, the relaxation of (I) across bovine ROS membrane vesicles without TPB is on the order of 60 s (Sundberg, 1983). The enhanced transport rate relative to egg PC vesicles is perhaps due to higher local dielectric constants within the bilayer structure due to the higher concentration of unsaturated centers and transmembrane proteins (rhodopsin). Castle and Hubbell (1976) estimated the half-time for transmembrane migration of (I) to be ~14 h in egg PC vesicles. If we take the dielectric constant to be 2.0 for the interior of this bilayer and assume the free energy of activation for transport to be the Born energy for the the ion in the membrane, the effective dielectric would have to increase

by only ~10% to produce the observed rate increase due to the above mentioned sources.

The experiments presented above were carried out on compositionally symmetric vesicles, and electrostatic asymmetry was created as a result of asymmetric, electrolyte screening. In native membrane systems, the more interesting situation of structural electrostatic asymmetry undoubtedly exists. In this case, a useful and simple experimental approach to assessing the asymmetry is to investigate the relaxation amplitude as a function of symmetric electrolyte screening with a permeable electrolyte like ammonium acetate. Fig. 8 *a* shows relaxation amplitudes, computed according to Eq. 4, and the Gouy-Chapman equation[4] as a function of symmetrical electrolyte for several different situations of charge asymmetry. The shape of the curve is a strong function of the charge asymmetry and provides an immediate qualitative assessment of the extent of asymmetry. Quantitative evaluation is accomplished by using the outer surface charge density determined from $t = 0$ data and fitting the curve using the inner charge density as a parameter. Alternatively, one can employ Eq. 10 to determine ϕ_i and the Gouy-Chapman Eq. to determine the inner charge density.

These approaches are currently being exploited to investigate charge distribution in photoreceptor membranes.

APPENDIX

In this appendix, we derive the general equation for the distribution function $\lambda(\infty)$ for permeable, charged ions in vesicles with equilibrium transmembrane potentials and charged interfaces. From this general expression, Eqs. 5, 6, and 10 are obtained.

The apparent equilibrium binding constants to the membrane interfaces are defined as

$$K_i' = \frac{N_{mi}/V_{mi}}{N_i/V_i} \quad \text{and} \quad K_o' = \frac{N_{mo}/V_{mo}}{N_o/V_o}, \tag{A1}$$

where the volumes and mole numbers are defined in the discussion of Fig. 3. In the presence of surface potentials

$$K_i' = K_i e^{-\phi_i} \quad \text{and} \quad K_o' = K e^{-\phi_o}, \tag{A2}$$

where K_i and K_o are the binding constants in the absence of a surface potential and ϕ_i, ϕ_o are the reduced (dimensionless) surface potentials defined in the text.

At electrochemical equilibrium,

$$\frac{N_i}{V_i} = \frac{N_o}{V_o} e^{-\Delta\phi_m}, \tag{A3}$$

where $\Delta\phi_m$ is the reduced transmembrane potential.

Now the total number of mols of bound ion is just

$$N_b(\infty) \equiv N_{mi}(\infty) + N_{mo}(\infty),$$

making use of Eqs. A1 and A3 we find

$$N_b(\infty) = N_{mo}(\infty)\left[1 + \frac{K_i}{K_o} \cdot \frac{V_{mi}}{V_{mo}} e^{-\Delta\phi_m}\right]. \tag{A4}$$

Similarly, for the total number of mols of free ions

$$N_f(\infty) = N_o(\infty) + N_i(\infty) = N_o(\infty)\left[1 + \frac{V_i}{V_o} e^{-\Delta\phi_m}\right]. \tag{A5}$$

Thus, from Eqs. A4 and A5

$$\lambda(\infty) = \frac{N_b(\infty)}{N_f(\infty)} = \lambda(0)\left[\frac{1 + (K_i'/K_o')(V_{mi}/V_{mo})e^{-\Delta\phi_m}}{1 + V_i/V_o e^{-\Delta\phi_m}}\right], \tag{A6}$$

where the identity

$$\lambda(0) \equiv \frac{N_b(0)}{N_f(0)} = \frac{N_{mo}(0)}{N_o(0)} = K_o \frac{V_{mo}}{V_o},$$

which follows from Eq. A1, has been used.

If the membranes are symmetric, $K_i = K_o$ and have no surface potentials ($\phi_i = \phi_o$) or transmembrane potentials ($\Delta\phi_m = 0$), Eq. A6 reduces to

$$\lambda(\infty) = \lambda(0) \frac{1 + V_{mi}/V_{mo}}{1 + V_i/v_o},$$

which is Eq. 5 of the text.

If the membranes are symmetric with no surface potentials, Eq. A6 can be solved for $\Delta\phi_m$ as

$$\Delta\phi_m = \ln\left[\frac{\lambda(0)(V_{mi}/V_{mo}) - \lambda(\infty)(V_i/V_o)}{\lambda(\infty) - \lambda(0)}\right],$$

which, when written in terms of $\Delta\phi_m$, is Eq. 6 of the text.

If the membranes are structurally symmetric ($K_i = K_o$) but have surface potentials ϕ_i and ϕ_o, not necessarily the same, Eq. A6 together with Eq. 7 from the text is reduced to

$$\ln\left[\lambda(\infty) - \frac{\phi(0)}{1 + V_i/V_o}\right] - \ln\left[\frac{\lambda'(0)(V_{mi}/V_{mo})}{1 + V_i/V_o}\right] + \phi_i = 0,$$

which is Eq. 10 of the text.

The values of λ used in the above Eqs. may be interpreted to be equal to that determined by EPR (Eq. 1) as long as the number of mols of (I) in the double layer is small compared to the number of mols of (I) in the bulk aqueous solutions. These conditions are met for the dilute vesicles and small surface potentials employed in the present experiments.

The authors would like to thank Dr. Christian Altenbach for a critical reading of the manuscript.

Funds for this research were provided by the National Institutes of Health grant #EY5216 and the Jules Stein Professor Endowment to W. L. Hubbell.

Received for publication 21 May 1985 and in final form 29 August 1985.

[4] For vesicles isolated from native membranes, typically larger than ~1,000 Å, the Gouy-Chapman equations for a planar surface are quite adequate.

REFERENCES

Bartlett, G.R. 1959. Phosphorus assay in column chromatography. *J. Biol. Chem.* 234:466–468.

Barton, P.G. 1968. The influence of surface charge density of phosphatides on the binding of some cations. *J. Biol. Chem.* 243:3884–3890.

Cafiso, D. S., and W. L. Hubbell. 1978*a*. Estimation of transmembrane potentials from phase equilibria of hydrophobic paramagnetic ions. *Biochemistry.* 17:187–195.

Cafiso, D. S., and W. L. Hubbell. 1978*b*. Estimation of transmembrane pH gradients from phase equilibria of spin-labeled amines. *Biochemistry.* 17:3871–3877.

Cafiso, D. S., and W. L. Hubbell. 1981. EPR determination of membrane potentials. *Annu. Rev. Biophys. Bioeng.* 10:217–244.

Cafiso, D. S., and W. L. Hubbell. 1982. Transmembrane electrical current of spin-labeled hydrophobic ions. *Biophys. J.* 39:263–272.

Castle, J. D., and W. L. Hubbell. 1976. Estimation of membrane surface potential and charge density from the phase equilibrium of a paramagnetic amphiphile. *Biochemistry.* 15:4818–4831.

Chabre, M., and A. Cavaggioni. 1973. Light induced changes of ionic flux in the retinal rod. *Nature New Biol.* 244:118–120.

Eisenberg, M., T. Gresalfi, T. Riccio, and S. McLaughlin. 1979. Adsorption of monovalent cations to bilayer membranes containing negative phospholipids. *Biochemistry.* 18:5213–5223.

Gaffney, B. J., and R. J. Mich. 1976. A new measurment of surface charge in model and biological lipid membranes. *J. Am. Chem. Soc.* 98:3044–45.

Huang, C., and J. T. Mason. 1978. Geometric packing constraints on egg phosphatidylcholine vesicles. *Proc. Natl. Acad. Sci. USA.* 75:308–310.

Hubbell, W. L., J. C. Metcalfe, S. M. Metcalfe, and H. M. McConnell. 1970. The interaction of small molecules with spin-labelled erythrocyte membranes. *Biochim. Biophys. Acta.* 219:415–427.

McLaughlin, S. 1977. Electrostatic potentials at membrane-solution interfaces. *Curr. Top. Membr. Transp.* 9:71–144.

McLaughlin, S., N. Mulrine, T. Gresalfi, G. Vaio, and A. McLaughlin 1981. Adsorption of divalent cations to bilayer membranes containing phosphatidylserine. *J. Gen. Physiol.* 77:445–473.

Ohshima, H., T. W. Healy, and L. R. White. 1982. Accurate analytic expressions for the surface charge density/surface potential relationship and double layer potential distribution for a spherical colloidal particle. *J. Coll. Interface Sci.* 90:17–26.

Singleton, W. S., M. S. Gray, M. L. Brown, and J. L. White. 1965. Chromatographic homogeneous lecithin from egg phospholipids. *J. Am. Oil Chem. Soc.* 42:53–56.

Stark, G. 1980. Negative hydrophobic ions as transport mediators for positive ions. *Biochim. Biophys. Acta.* 600:233–237.

Sundberg, S. A. 1983. An ESR method for the investigation of asymmetric electrostatic properties in liposomes and bovine photoreceptor membranes. Ph.D. thesis, University of California, Berkeley.

Waggoner, A. S. 1979. Dye indicators of membrane potential. *Annu. Rev. Biophys. Bioeng.* 8:47–68.